

# Flux rate effects in the erosive wear of elastomers

J. C. ARNOLD, I. M. HUTCHINGS

*University of Cambridge, Department of Materials Science and Metallurgy, Pembroke Street, Cambridge CB2 3QZ, UK*

The variation of erosion rate with particle flux was studied for five elastomers (natural rubber and epoxidized natural rubber, both with and without antioxidant, and butyl rubber) whilst subject to erosion by 120  $\mu\text{m}$  silica particles at 50  $\text{m sec}^{-1}$ . The erosion rate was found to increase at low particle fluxes, for the elastomers without antioxidant. Infrared spectroscopy showed that there was a considerable degree of oxygen incorporation into the elastomer surface during erosion. Studies with an intermittent erosion stream suggest that a transient reaction occurs on impact causing degradation of the elastomer surface, which can account for the variation of erosion rate with particle flux. Studies with a range of erodent particles (silica, alumina, silicon carbide and soda-lime glass beads) showed that the degradation is more pronounced for hydrophilic particles.

## 1. Introduction

Elastomers have been shown in some situations to provide good resistance to wear by the impact of small hard particles [1], though the mechanisms of erosion are still unclear. Of the many variables that influence the erosion resistance of elastomers, the particle flux is of particular interest, defined as the mass of particles impacting per unit time per unit area.

The flux is found to have little influence on the erosion rate (defined as the mass of surface material removed per unit mass of impinging particles) for metals and ceramics [2]. There is some evidence, however, that particle flux has a stronger effect on erosion rate for elastomers [3]. It is important to explore this effect, because most laboratory investigations of erosion are carried out at much higher particle fluxes than are encountered in practical applications; in order to apply the results of laboratory testing in practice, an understanding of the influence of flux is essential.

Bartenev and Penkin [4] found that the erosion rate of styrene-butadiene rubber, chloroprene rubber and steel decreased as the particle flux increased above 100  $\text{kg m}^{-2} \text{sec}^{-1}$ . They attributed this effect to collisions between incoming particles and those rebounding from the target surface. Some incoming particles subject to such collisions will be deflected away from the target surface without hitting it, causing the measured erosion rate to be reduced. As the flux is increased, the likelihood of such collisions is increased and so the erosion rate will be lowered. A detailed analysis of the probability and effect of collisions has been performed by Andrews and Horsfield [5].

Marei and Izvozhikov [6] proposed an erosion mechanism for elastomers involving a build-up of strain on the surface due to incomplete strain relaxation between impacts. They suggested that the strains produced by a single impact are insufficient to cause

material removal, and that several successive impacts are necessary to raise the strain to a sufficient level to cause material removal. This mechanism would explain the greater erosion resistance observed for more resilient elastomers [4, 7-9]. It should also lead to a marked dependence of erosion rate upon flux. As the flux is increased, the time between impacts will be reduced, causing more strain accumulation, leading to a greater erosion rate.

Uemois and Kleis [3] found several effects of particle flux upon erosion. The erosion rates of mild steel and a cermet decreased as the flux increased over a range from 10 to 2000  $\text{kg m}^{-2} \text{sec}^{-1}$ . This effect, which was more marked at higher impact velocities, at normal incidence and with smaller particles, can be attributed to collisions between particles. A variable effect was found for rubber: at low velocities and at glancing incidence, the erosion rate of rubber decreased as the flux was increased from 500 to 5000  $\text{kg m}^{-2} \text{sec}^{-1}$ , again probably due to particle collisions. For higher velocities and at normal incidence, the erosion rate increased over the flux range 1000 to 10 000  $\text{kg m}^{-2} \text{sec}^{-1}$ .

Andrews [10] concluded from a theoretical analysis of erosion that the flux will affect erosion only when it causes a temperature increase, leading to mechanical softening or surface melting. Walley and Field [11] calculated the flux at which temperature effects would become important in the erosion of polyethylene to be about 180  $\text{kg m}^{-2} \text{sec}^{-1}$ . Their calculation assumed that conduction through the sample would be the main heat-dissipating mechanism, and neglected convection to the rapidly moving air stream. No effects of flux were found in their experimental tests over the range from 5 to 22  $\text{kg m}^{-2} \text{sec}^{-1}$ . Hutchings *et al.* [7] also found no effects of flux on the erosion rate of epoxidized natural rubber (containing antioxidant) at low flux levels (2 to 8  $\text{kg m}^{-2} \text{sec}^{-1}$ ).

One further mechanism which could cause a variation of erosion rate with flux is environmental degradation. For a given mass of erodent, erosion at low flux involves longer time scales than erosion at high flux, giving more opportunity for any time-dependent processes such as oxidation or ozonation to occur. Environmental conditions are known to affect the abrasion [12, 13] and fatigue [14, 15] of rubber, and as a fatigue mechanism has been proposed for the erosion of elastomers [4, 16] the influence of environmental conditions could be important.

The aim of the present work was to determine the variation of erosion rate with flux at low particle fluxes for several elastomers. As it became clear from preliminary work that ageing processes were playing an important role in the observed erosion behaviour, a detailed study of these was made.

## 2. Experimental method

Samples of three base elastomers were prepared at the Malaysian Rubber Producers' Research Association (M.R.P.R.A., Brickendonbury, Hertford), in the form of unfilled vulcanized sheets 5 mm thick. The elastomers used were natural rubber (high resilience) with and without Nonox ZA antioxidant (NR(+)) and NR(-) respectively), epoxidized natural rubber (low resilience) with and without antioxidant (ENR50(+)) and ENR50(-)), and butyl rubber (low resilience, IIR), known for its good resistance to oxidation. The compositions and curing conditions of these elastomers are given in Table I.

Test specimens 20 mm × 40 mm in size were cut from the rubber sheets and fixed to steel backing plates in a relaxed condition. They were eroded with silica sand of 120 μm mean particle size in a gas-blast erosion apparatus, as described previously [7]. This method allows easy control of the impact parameters such as velocity, impact angle and particle flux. The velocity of impact used in all experiments was measured by the double-disc method [17].

The wear was measured by weighing the specimens to within ± 50 μg, after erosion by a fixed mass of sand. Most samples showed an incubation period before the onset of steady-state erosion, and the erosion rate was calculated from a plot of cumulative mass loss against mass of sand, once the incubation period had been passed. Before weighing, erodent particles on the surface were removed by an air-blast.

Infrared (IR) spectra of the surfaces were taken using a Perkin-Elmer 882 spectrometer by a reflection

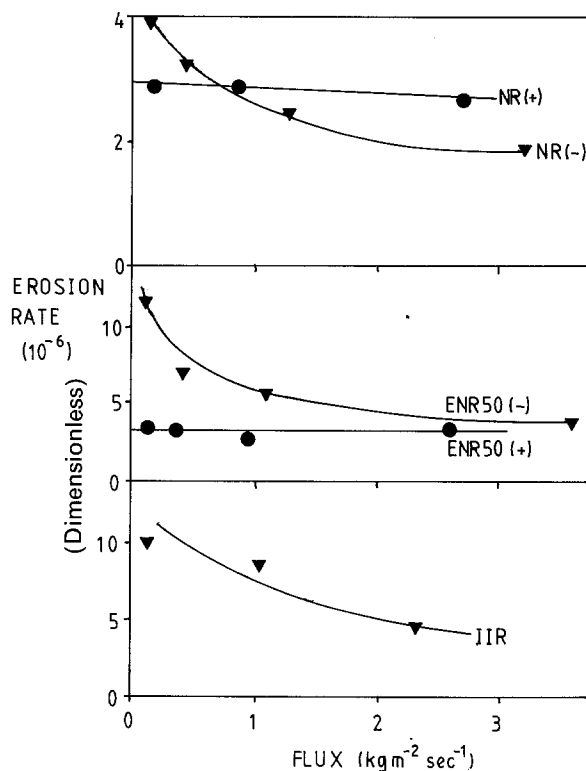


Figure 1 The variation of erosion rate with particle flux for the five elastomers tested. The erodent was 120 μm silica particles at an impact velocity of 50 m sec<sup>-1</sup> and an impact angle of 30°.

technique. The absorbances of the peaks were measured relative to the baseline of maximum transmission, which was lower than 100% for this experimental method due to internal reflection losses. The peak absorbances were then compared with that of the CH<sub>2</sub> bending peak as an internal standard [18]. Thus, for example, the relative absorbance for the O-H peak (3400 cm<sup>-1</sup>) was obtained as follows:

$$A(\text{O-H}) = \frac{\text{Absorbance of O-H peak relative to baseline}}{\text{Absorbance of CH}_2 \text{ peak relative to baseline}}$$

To investigate the effect of interrupting the stream of erodent particles, an eight-segmented shutter was used, rotated at a constant speed between the nozzle of the erosion apparatus and the sample, thus providing bursts of erosive particles with a mark/space ratio of 1:1. The erosion rate of ENR50(-) was measured at normal incidence with the shutter operating at various frequencies. It was assumed that with the shutter operating, half the amount of erodent passing through

TABLE I Compositions of the elastomer samples tested

| Designation | Base rubber        | Additive (p.p.h.* base rubber) |              |         |     |          |                  |     |     |      | Cure conditions |                  |
|-------------|--------------------|--------------------------------|--------------|---------|-----|----------|------------------|-----|-----|------|-----------------|------------------|
|             |                    | ZnO                            | Stearic acid | Sulphur | CBS | Nonox ZA | Sodium carbonate | MOR | MBT | TMTD | Time (min)      | Temperature (°C) |
| NR(-)       | Natural            | 5                              | 2            | 2.5     | 0.6 | -        | -                | -   | -   | -    | 40              | 140              |
| NR(+)       | Natural            | 5                              | 2            | 2.5     | 0.6 | 2        | -                | -   | -   | -    | 40              | 140              |
| ENR50(-)    | Epoxidized natural | 5                              | 2            | 1.2     | -   | -        | 0.2              | 1.2 | -   | -    | 35              | 140              |
| ENR50(+)    | Epoxidized natural | 5                              | 2            | 1.2     | -   | 2        | 0.2              | 1.2 | -   | -    | 35              | 140              |
| IIR(-)      | Butyl              | 5                              | 1            | 2       | -   | -        | -                | -   | 1   | 1    | 60              | 160              |

\*Parts per hundred.

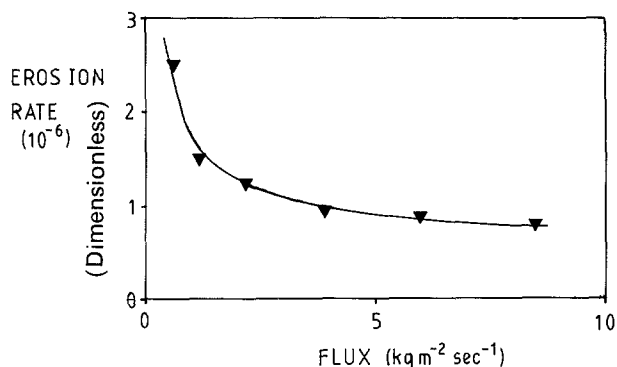


Figure 2 The variation of erosion rate with particle flux for ENR50(-) with  $120 \mu\text{m}$  silica particles at an impact velocity of  $50 \text{ m sec}^{-1}$  and an impact angle of  $90^\circ$ .

the apparatus was deflected away from the sample by the shutter. The mass of sand hitting the sample was therefore half the amount passing through the apparatus, and the erosion rate calculated from the mass loss was adjusted to take this into account.

### 3. Results

The variation of erosion rate with flux at an impact angle of  $30^\circ$  and a particle velocity of  $50 \text{ m sec}^{-1}$  for all five elastomers tested is shown in Fig. 1. A similar behaviour was observed for the samples eroded at normal incidence, as seen in Fig. 2 for ENR50(-).

All the samples exhibited an incubation period, which was of greater extent at normal incidence than at an impact angle of  $30^\circ$ . The incubation period was accompanied by a mass gain, which can be attributed to erodent particles embedding in the sample surface. The eroded areas of all the samples were observed to darken in colour during the incubation period. The darkening was more pronounced for the elastomers without antioxidant than for those with antioxidant. The darkened area was not affected by ultrasonic cleaning of the sample in acetone, showing that the effect was not due to embedded silica particles.

The relative IR absorbances of the O-H, C=O and C-O stretching frequencies were measured for NR(-) in the uneroded, eroded, abraded and thermally oxidized states, and the values are shown in Fig. 3. The abraded sample was prepared by rubbing the surface with 120 mesh dry SiC paper. The thermally oxidized samples were prepared by heating in a dark oven at  $130^\circ \text{C}$  for times from 4 to 24 h.

Spectra of uneroded, eroded and thermally oxidized

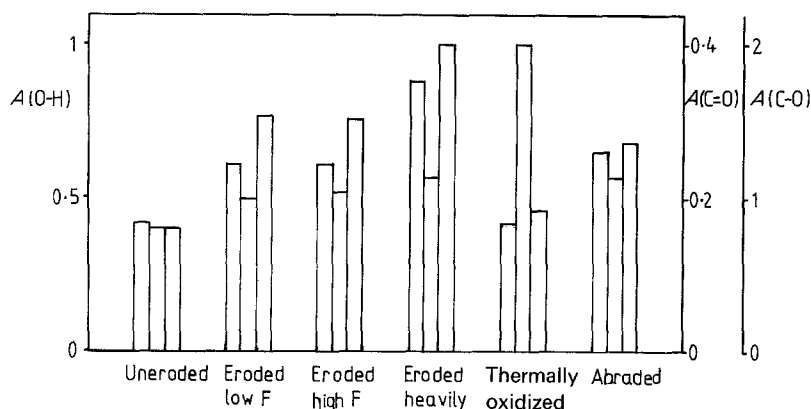


Figure 3 The relative O-H, C=O and C-O absorbances for NR(-).

TABLE II Impurity content (wt %) of the eroded surfaces of NR(-) samples after erosion by a range of erodent particles

| Impurity | Erodent     |        |         |                 |
|----------|-------------|--------|---------|-----------------|
|          | Glass beads | Silica | Alumina | Silicon carbide |
| Si       | 2.4         | 6.0    | 1.1     | 9.2             |
| Al       | —           | 1.8    | 15.5    | 1.3             |
| Fe       | 0.9         | 4.9    | 5.0     | 12.0            |
| Cu       | 0.5         | 1.1    | 1.0     | 3.7             |
| Ni       | 0.1         | 0.3    | 0.8     | 2.1             |
| Cr       | 0.2         | 0.5    | 1.0     | 3.0             |
| Ti       | 0.2         | 0.2    | 1.4     | 0.2             |

samples of NR(+) were also taken and the relative absorbances are shown in Fig. 4.

The erosion rate of NR(-) was also measured using nitrogen as the propellant gas, and was found to be identical to that found using compressed air. The IR spectrum of the surface was also found to be the same as for erosion in air.

To investigate the part played by the nature of the erodent, ENR50(-) was eroded at high and low flux with glass beads, silica particles, alumina particles, all of  $150 \mu\text{m}$  diameter and with  $100 \mu\text{m}$  silicon carbide particles. Fig. 5 shows the observed erosion behaviour. The IR spectra of samples of NR(-) eroded with each erodent were taken, and values of the relative C-O absorbances are shown in Fig. 6. Energy dispersive X-ray analysis (EDX) was performed on the samples after erosion with each erodent. The impurity concentrations are given in Table II.

The erosion rate of ENR50(-) was measured with an interrupted particle stream under conditions of normal impact. A considerable increase in erosion rate was observed under intermittent conditions with an interruption frequency of 40 Hz, compared with continuous erosion (Fig. 7). By varying the frequency of rotation of the shutter, the difference between intermittent and continuous erosion rates was measured for erosive burst times varying from 0.01 to 1 sec (Fig. 8).

The eroded samples were examined by scanning electron microscopy. Typical surface morphologies for an impact angle of  $30^\circ$  are shown in Fig. 9. The features are similar to those found in previous studies [7] with transverse ridges on the scale of about  $20 \mu\text{m}$  visible in the highly resilient NR, and a more randomly broken surface with little or no directionality in the much less resilient ENR50. There was little or no

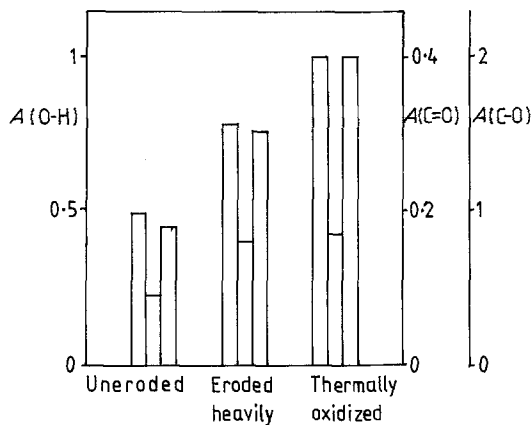


Figure 4 The relative O-H, C=O and C-O IR absorbances for NR(+).

observable difference between the eroded surface features of the elastomers with and without antioxidant.

#### 4. Discussion

There was a substantial increase in the erosion rates of the elastomers without antioxidant as the flux was decreased. This effect was largely eliminated for the elastomers containing antioxidant, though somewhat surprisingly the butyl rubber (IIR), which is more resistant to thermal oxidation, showed similar behaviour to the NR(-) and ENR50(-). It should be noted that the samples of NR(+) were tested at a slightly higher impact velocity than the other samples; the higher erosion rate observed for this elastomer than for the NR(-) at high flux is not therefore significant.

There are several possible explanations for the observed increase in erosion rate at low flux. Particle

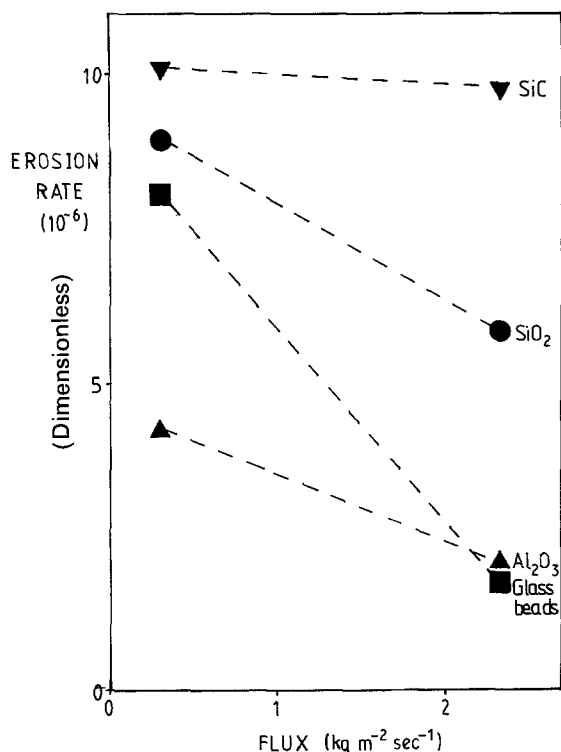


Figure 5 The variation of erosion rate with flux for ENR50(-) with a range of erodent particles. The particle impact velocity was between 46 and 50  $\text{m sec}^{-1}$ , at an impact angle of 30°.

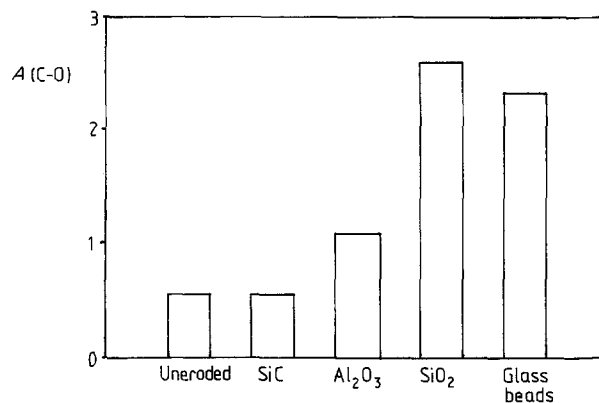


Figure 6 The relative C-O IR absorbances for NR(-) eroded with a range of erodent particles.

interaction effects might possibly be causing a reduction in erosion rates at high fluxes. The probability of collisions in the erosion stream can, however, be calculated [5], and proves to be negligibly small, even at the highest fluxes used. Another possibility is that as the flux increases, the surface temperature increases, which might cause a reduction in erosion rate [6]. A thermocouple embedded less than a millimetre below the target surface showed no significant temperature change, and calculations based on heat transfer by convection to the air stream show that any bulk temperature rise will have been less than 1 K. The fact that the observed effects of flux are largely eliminated in the elastomers with antioxidant suggests that environmental degradation is the cause. This suggestion is supported by the darkening of the surface of the samples, an effect which was also reduced by the addition of antioxidant.

The IR spectra of the natural rubber samples also show evidence of environmental degradation. The oxidation of natural rubber has been studied extensively in the past by IR spectroscopy. It has been shown generally that as thermal oxidation occurs, the absorption of the O-H peak ( $3400 \text{ cm}^{-1}$ ), the C=O peak ( $1720 \text{ cm}^{-1}$ ) and the C-O peaks ( $900$  to  $1300 \text{ cm}^{-1}$ ) all increase [19, 20]. Various hydroxyl, carbonyl, carboxyl, ester, ether, and peroxide groups are formed by the oxidation reaction [21, 22], and it is an increase in the concentration of these groups that is detected by IR spectroscopy.

It can be seen from the absorbances of the peaks of interest (Fig. 3) that a large degree of oxygen incorporation accompanies the erosion of the NR(-). There is a large increase in the O-H and C-O absorbances with the degree of erosion, coupled with a slight increase in the C=O absorbance. The thermally oxidized sample, however, shows a large increase in the C=O absorbance, with only slight increases in the O-H and C-O absorbances. It would seem, therefore, that the degradation reaction associated with erosion is of a different character from thermally induced oxidation. The shape of the hydroxyl peak for the eroded samples is unlike that for the thermally oxidized sample, with a small subsidiary peak at a slightly higher wavenumber. This could be due to the presence of hydroperoxide groups, which at high temperatures would have decomposed, and which would

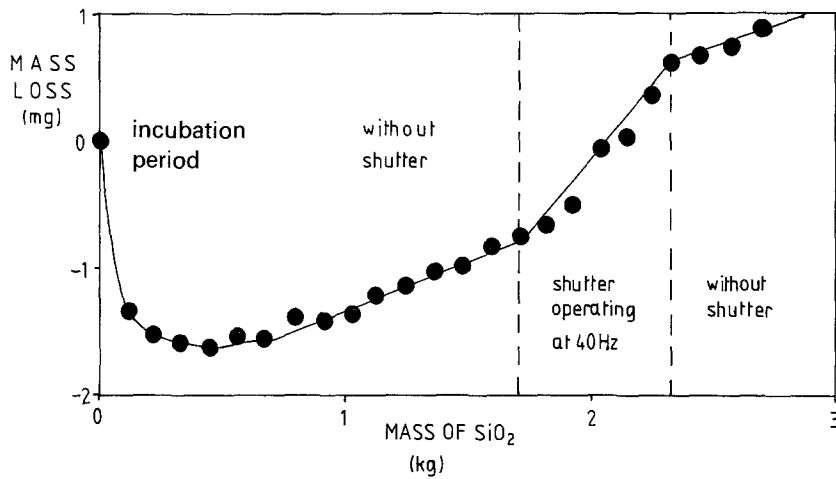


Figure 7 A plot of specimen mass loss against mass of silica striking the surface of an ENR50(-) specimen. The particle impact velocity was  $50 \text{ m sec}^{-1}$  at an impact angle of  $90^\circ$ . Intermittent erosion conditions were operating for part of the test.

also explain the absence of a large number of  $\text{C}=\text{O}$  groups in the eroded samples.

In previous work, the character of the oxidation reaction has been found to vary, depending on the catalytic environment. Golub *et al.* [18] found differences between thermal and photosensitized oxidation. Kusminsky [23], in a review of fatigue, found the character of the oxidation process to be altered in the presence of stress.

It is interesting to note that the sample abraded in air showed a very similar spectrum to the eroded samples. This suggests that the chemical degradation process occurring during abrasion is similar to that found with erosion.

The samples of natural rubber with antioxidant give spectra which show an increase in the amounts of  $\text{O}-\text{H}$  and  $\text{C}-\text{O}$  groups, with a small increase in the amount of  $\text{C}=\text{O}$  groups.

The erosion and IR results obtained with nitrogen as the accelerating gas suggest exactly the same degree of chemical degradation as those found with compressed air. The erosion rate of ENR50(-) measured at low flux was not reduced when nitrogen was used, and the IR spectrum of NR(-) showed the same amount of oxygen incorporated into the surface for both carrier gases.

The differences observed by varying the erodent particles are of considerable importance. Both the extent of the variation of erosion rate with flux and the degree of degradation of the surface as determined by IR spectrometry were lower with alumina than with silica, and both were virtually eliminated with silicon carbide. Glass beads gave similar behaviour to that

observed with silica. It would seem, therefore, that the degradation of the elastomer surface is caused by some interaction with the erodent particle surface. This interaction may possibly involve water adsorbed on the surface of the particles, because this is an important difference in the characteristics of the three erodents used. Silica and glass, with a large amount of adsorbed water, cause extensive degradation; alumina, with a smaller amount of adsorbed water, causes less degradation, and silicon carbide, which is virtually free from adsorbed water, has a negligible effect. The EDX results (Table II) show that the amount of impurities transferred to the rubber surface from the erodent is not important. The transition metal impurities originate either from the erodent particles themselves or from the inner surface of the erosion apparatus, worn away by the erodent.

It is suggested that a very local and rapid reaction occurs during erosion after each impact. The next impact on the same region then strikes an area which is more susceptible to mechanical damage as a result of this reaction. Such a mechanism would explain the variation of erosion rate with flux observed in this work. As the flux is increased, the time between impacts on one particular surface site is decreased. The degradation reaction will then have less time to occur before the next impact, and so the degree of degradation and hence the amount of erosion will be reduced. The process can be viewed as a series of transient reactions occurring after each impact. At high fluxes, these transients overlap to a greater degree than at low fluxes; the amount of degradation per impact is therefore reduced at high fluxes. At very high

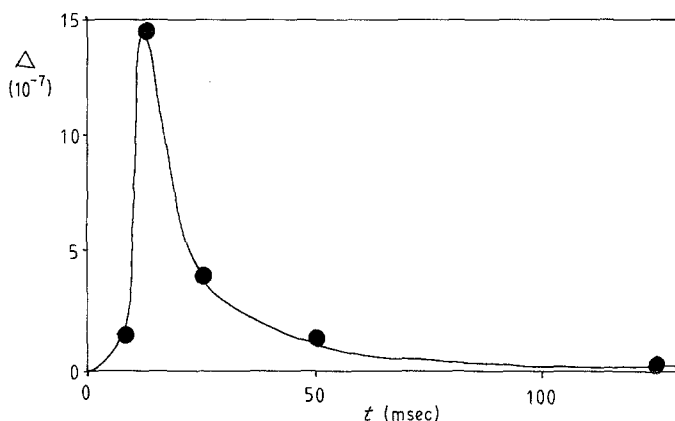


Figure 8 The variation of the difference,  $\Delta$ , between the erosion rate under intermittent conditions and that under continuous conditions, with the erosive burst time for ENR50(-) at an impact angle of  $90^\circ$ .

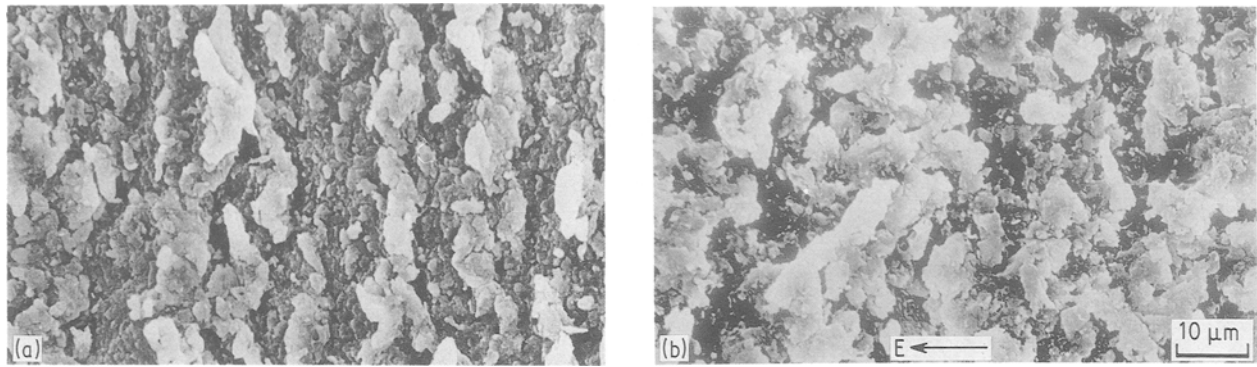


Figure 9 Scanning electron micrographs of the surfaces of the rubber samples after erosion at 30° impact angle. (a) NR(+), (b) ENR50(+). E indicates the erosion direction.

flux levels, the transients will overlap to such an extent that virtually no degradation effect is seen.

The results of the intermittent erosion tests support this proposed mechanism. If a burst of erosion at a relatively high flux is followed by a period with no particle impacts, then the impacts that occur just before the end of the burst will give rise to an extended period of degradation during the quiescent period. The first impacts occurring after the interruption will then strike a more heavily degraded surface and lead to more damage than if they had followed closely after the preceding impacts. A higher rate of erosion would, therefore, be expected with an intermittent erosion stream, as is indeed seen in Fig. 7. The erosion rate observed with the shutter operating at 40 Hz (giving an erosive burst time of 12.5 msec) is greater, after correction for the smaller mass of erodent striking the sample, than the continuous erosion rate observed both before and after the period of intermittent erosion.

The difference between intermittent and continuous erosion rates depends on the timescale of the erosive burst. As the erosive burst time is decreased (i.e. with increasing shutter frequency), the difference in erosion rate rises to a maximum value for a time interval of about 12 msec, followed by a subsequent decrease at shorter times. This variation can be explained in a qualitative manner in the following way. With long erosive burst times, the number of impacts leading to an extended period of degradation will be only a very small fraction of the total number, and so the extra mass loss due to chemically enhanced erosion will be negligible. With very short erosive burst times, on the other hand, the time between bursts of erosion will be too short for any appreciable chemical degradation to occur. At the shortest timescales, the situation will effectively be the same as erosion by a continuous stream with half the flux.

Any theoretical model for the variation of erosion rate with burst time would have to take account of the distributions of impacts with respect to both time and position, and is beyond the scope of the present study. The position of the maximum can, however, provide an indication of the area affected by each impact. The area of the impact site can be calculated from

$$F = \frac{M_p N}{a}$$

where  $F$  is the particle flux,  $M_p$  is the mass of each

particle,  $N$  the number of impacts per second per impact site, and  $a$  the area of the impact site. A simple model, assuming a uniform distribution of impacts and an exponentially decaying transient reaction, predicts that the maximum erosion will occur when approximately three impacts occur per impact site in each erosive burst. If three impacts occur in a time of 12.5 msec (corresponding to the shutter frequency of 40 Hz for maximum erosion), then the area affected by each impact must be approximately 300 to 350  $\mu\text{m}$  in diameter. This is considerably larger than the particle diameter (120  $\mu\text{m}$ ).

The process occurring immediately after each impact is probably a very rapid and local reaction, possibly involving water adsorbed on the erodent particle, which results in mechanical weakening of the area around the impact site. The reaction is likely to involve free radicals, the formation of which is strongly catalysed by the mechanical deformation and high temperatures [23, 24] which will be present locally at an impact site. The fact that butyl rubber also shows signs of degradation, despite its resistance to thermal oxidation, can be explained. Being fully saturated, butyl rubber has no double bonds to act as favourable sites for radical formation and oxidative attack, under normal conditions. Double bonds may not, however, be needed for free radical formation under erosive attack because of the high mechanical and thermal energies associated with each impact.

## 5. Conclusions

The erosion rate of elastomers is seen to increase with decreasing flux at low flux levels. This increase is suppressed by the incorporation of Nonox ZA anti-oxidant into the rubber.

IR studies show that there is a considerable amount of oxygen incorporation into the surface of the eroded elastomers. This incorporation is of a different nature from that accompanying thermal oxidation.

It is suggested that there is a local reaction triggered by impact, which causes mechanical degradation of the elastomer surface. This reaction is shown by intermittent erosion tests to be of a transient nature, thus leading to the observed variation of erosion rate with flux.

There is a correlation between the magnitude of the apparent degradation and the amount of water adsorbed on the erodent particles; impurities transferred to the

elastomer from the erodent particles do not seem to play a significant role.

### Acknowledgements

This work was supported by the SERC and the Malaysian Rubber Producers' Research Association via a CASE studentship. We are grateful to Dr K. N. G. Fuller and Dr A. H. Muhr for helpful discussions and advice.

### References

1. V. K. AGARWAL, D. MILLS and J. S. MASON, "A comparison of the erosive wear of steel and rubber bends in pneumatic conveying system pipelines", Proceedings 6th International Conference on Erosion by Liquid and Solid Impact, edited by J. E. Field and N. S. Corney, Cavendish Laboratory, Cambridge, paper 60 (Cavendish Laboratory, Cambridge, 1983).
2. A. W. RUFF and S. M. WIEDERHORN, *Treatise Mater. Sci. Technol.* **16** (1979) 69.
3. H. UUEMOIS and I. KLEIS, *Wear* **31** (1975) 359.
4. G. M. BARTENEV and N. S. PENKIN, *Sov. J. Friction Wear* **1** (1980) 584.
5. D. R. ANDREWS and N. HORSFIELD, *J. Phys. D* **16** (1983) 525.
6. A. I. MAREI and P. V. IZVOZCHIKOV, "Determination of the wear of rubbers in a stream of abrasive particles", in "Abrasion of Rubber", edited by D. I. James (McLaren, London, 1967) pp. 274-80.
7. I. M. HUTCHINGS, D. W. T. DEUCHAR and A. H. MUHR, *J. Mater. Sci.* **22** (1987) 4071.
8. P. V. RAO and D. H. BUCKLEY, "Spherical microglass particle impingement studies of thermoplastic materials at normal incidence", NASA technical memorandum 83410 (1983).
9. R. E. MORRIS and J. OSER, *Rubber Age* **92** (1963) 96.
10. D. R. ANDREWS, *J. Phys. D* **14** (1981) 1979.
11. S. M. WALLEY and J. E. FIELD, *Phil. Trans. Roy. Soc. Lond.* **A321** (1987) 277.
12. A. SCHALLAMACH, *J. Appl. Polym. Sci.* **12** (1968) 281.
13. Y. UCHIYAMA, *Wear* **110** (1986) 369.
14. A. N. GENT, *J. Appl. Polym. Sci.* **6** (1962) 497.
15. G. J. LAKE, "Aspects of Fatigue and Fracture in Rubber", in "Progress of Rubber Technology" (Applied Science, London, 1983) pp. 89-143.
16. S. SODERBERG, S. HOGMARK, U. ENGMAN and H. SWAHN, *Tribology Int.* **14** (1981) 333.
17. A. W. RUFF and L. K. IVES, *Wear* **35** (1975) 195.
18. M. A. GOLUB, M. L. ROSENBERG and R. V. GEMMER, "Photosensitised oxidation of polyisoprene", in "Applications of Polymer Spectroscopy", edited by E. G. Brame (Academic, London, 1978) pp. 87-99.
19. G. SALOMON and A. C. VAN DER SCHEE, *J. Polym. Sci.* **14** (1954) 181.
20. J. E. FIELD, D. E. WOODFORD and S. D. GEHTMAN, *ibid.* **15** (1955) 51.
21. F. HILTON, *Trans. Inst. Rubber Ind.* **17** (1942) 319.
22. R. F. NAYLOR, *ibid.* **20** (1944) 45.
23. A. S. KUSMINSKY, "Fatigue resistance and antifatigue agents in elastomers", in "Development of Polymer Stabilisation 4", edited by G. Scott (Applied Science, London, 1981) pp. 71-111.
24. J. HRIVIKOVA, A. BLAZKOVA and L. LAPCIK, *J. Appl. Polym. Sci.* **25** (1980) 761.

Received 19 February  
and accepted 14 June 1988